REVISION 3

Coexisting pseudobrookite, ilmenite and titanomagnetite in hornblende andesite of the Coleman Pinnacle flow, Mount Baker, Washington, and the effect of high oxygen fugacity

Emily K. Mullen[1,*] and I. Stewart McCallum[2]

[1]Pacific Centre for Isotopic and Geochemical Research, Department of Earth and Ocean Sciences, University of British Columbia, Vancouver, B.C. V6T1Z4, Canada.

[2]Department of Earth and Space Sciences, Box 351310, University of Washington, Seattle, Washington 98195, U.S.A.

*contact: emullen@eos.ubc.ca

ABSTRACT

Pseudobrookite microphenocrysts occur in cognate inclusions in the ~305 ka Coleman Pinnacle hornblende andesite flow from the Mount Baker volcanic field, WA. Pseudobrookites are associated with hornblende phenocrysts and glomerophyric clusters of orthopyroxene, clinopyroxene, plagioclase, ilmenite, titanomagnetite, apatite and zircon in a matrix of fresh rhyolitic glass. Grains of pseudobrookite are rimmed by or intergrown with ilmenite. These textures are analogous to those observed between armalcolite and ilmenite in high-Ti lunar basalts. In a unique occurrence, pseudobrookite and titanomagnetite form a symplectitic intergrowth surrounding a core of ilmenite. Mass balance calculations show that the pseudobrookite + titanomagnetite assemblage is not an isochemical decomposition of ilmenite.

Always consult and cite the final, published document. See http://www.minsocam.org or GeoscienceWorld

In the TiO_2–FeO–Fe_2O_3 system (Mg-free), pseudobrookite and titanomagnetite solid solutions do not coexist. However, all three Fe-Ti oxides in the symplectitic assemblage contain significant amounts of Mg. In the TiO_2–MgO–FeO–$FeO_{1.5}$ system at high oxygen fugacities, the Mg-rich pseudobrookite + titanomagnetite assemblage is stable relative to the conjugate pair of Mg-bearing ilmenite solid solutions. At lower f_{O2}, Fe^{2+} increases, Mg/(Mg+Fe^{2+}) decreases and the conjugate ilmenite pair becomes the stable assemblage at Mg# less than ~0.6. The compositions of coexisting ilmenite + titanomagnetite pairs in the Coleman Pinnacle andesite yield T = 900-1000°C and f_{O2} = NNO + 1.5 to + 1.75, one of the highest redox states on record for arc magmas. The calculated f_{O2} range is consistent with the composition of the ilmenite in equilibrium with pseudobrookite ± rutile and with Fe^{3+}-rich cores in hornblende phenocrysts.

Keywords: Pseudobrookite, ilmenite, titanomagnetite, oxygen fugacity, andesite, Mount Baker.

INTRODUCTION

The compositions of coexisting ilmenite–hematite and ulvöspinel–magnetite solid solutions, hereafter referred to as ilmenite and titanomagnetite, respectively, have been widely used as a geothermometer/oxybarometer in magmatic systems following the initial calibration of Buddington and Lindsley (1964). The third solid solution in the TiO_2–MgO–FeO–$FeO_{1.5}$ system is pseudobrookite, which has an ideal end member formula of $Fe_2^{3+}TiO_5$ and encompasses the compositional range extending to $Fe^{2+}Ti_2O_5$ and $Fe_2MgTi_3O_{10}$ (Bowles, 1988). For brevity in some figures and tables, we refer to $Fe^{2+}Ti_2O_5$ as "ferropseudobrookite" and $MgTi_2O_5$ as "karrooite" (following Lindsley, 1991) although we recognize that these names have been discredited (Bowles, 1988). Compositions extending further toward $MgTi_2O_5$ are known as

Always consult and cite the final, published document. See http://www.minsocam.org or GeoscienceWorld

armalcolite, which has the ideal formula $Fe^{2+}_{0.5}Mg_{0.5}Ti_2O_5$. Pseudobrookites commonly also contain minor amounts of aluminum and manganese.

Pseudobrookite is much less common in terrestrial volcanic rocks than ilmenite and titanomagnetite. Microphenocrysts relatively rich in the $FeTi_2O_5$ end member occur in the early phases of the 1955 basalt eruption along the lower east rift zone of Kilauea volcano (Anderson and Wright, 1972). The pseudobrookite grains are rimmed by ilmenite and embedded in a glassy matrix, indicating a reaction relationship between pseudobrookite and melt. Titanomagnetite phenocrysts also occur in the 1955 basalt. Pseudobrookite coexisting with titanomagnetite has also been reported in alkalic basalts from Gough Island (Le Roex, 1985), in tinguaite and syenite dikes at Katzenbuckel volcano, Germany (Stähle and Koch, 2003), in ultrapotassic basanites and basalts from the central Sierra Nevada (van Kooten, 1980) and in an alkalic gabbro from Kauai, Hawaii (Johnston and Stout, 1984). Insofar as textural details are not provided for the Gough and Sierra Nevada occurrences, it cannot be unequivocally established that they represent equilibrium assemblages. The Hawaiian occurrence shows highly acicular pseudobrookite (referred to as "kennedyite" by Johnston and Stout, 1984) associated with euhedral magnesioferrite, euhedral salite, and acicular "swallow-tail" olivine in an oligoclase-rich matrix. Very high Fe^{3+} contents in all ferromagnesian phases attest to the extremely oxidized nature of the parent magma. At the Katzenbuckel locality, primary pseudobrookite in the tinguaite dike is partly replaced by ilmenite or by fine myrmekitic intergrowths of hematite, ilmenite and magnetite (Stähle and Koch, 2003). Pseudobrookite and titanomagnetite coexisting in a syenite vein is interpreted by Stähle and Koch (2003) as a secondary assemblage replacing primary ilmenite.

Always consult and cite the final, published document. See http://www.minsocam.org or GeoscienceWorld

Pseudobrookite occurs most commonly as a secondary mineral in assemblages formed at the most advanced stage (C7) of oxidation of ilmenite and/or spinel (Haggerty, 1991a) where it is associated with hematite and rutile. Secondary pseudobrookite typically occurs as pseudomorphic {111} lamellae or as graphic intergrowths with hematite.

In the Coleman Pinnacle hornblende andesite flow of the Mt. Baker volcanic field, pseudobrookite microphenocrysts rimmed by or intergrown with ilmenite occur in glomerophyric clusters. Such textures are analogous to those between armalcolite and ilmenite in lunar basalts (Anderson et al., 1970). In an unusual occurrence, pseudobrookite and titanomagnetite, a rare assemblage in natural systems, forms a symplectitic intergrowth surrounding a core of ilmenite. Substantial Mg is present in all Fe-Ti oxides in the Coleman Pinnacle flow, and subequal amounts of Fe^{2+} and Mg in the pseudobrookite indicate compositions intermediate between the ideal armalcolite ($Mg_{0.5}Fe_{0.5}Ti_2O_5$) and pseudobrookite (Fe_2TiO_5) end-member compositions. The elevated $Mg/(Mg+Fe^{2+})$ is partly a consequence of the high oxygen fugacity (high $Fe^{3+}/\Sigma Fe$) of the magma.

GEOLOGIC SETTING

Mt. Baker is an andesitic stratovolcano of the Cascade arc, located ~50 km east of Bellingham, WA. The modern Mt. Baker cone has been active for the past ~40 ka and is the most recent product of the areally extensive Mt. Baker volcanic field that over the past 1.3 Ma has erupted lavas and ash-flows ranging in composition from basalt to rhyolite (Hildreth et al., 2003). The Coleman Pinnacle andesite is one of several flows that erupted along the margins of, and within, the 1.15 Ma Kulshan Caldera. A glaciated remnant of the andesite is preserved ~10 km northeast of the summit of Mt. Baker (Fig. 1). The flow has been dated at ~305 ka (Ar-Ar

Always consult and cite the final, published document. See http://www.minsocam.org or GeoscienceWorld

age) (Hildreth et al. 2003) and is the only pseudobrookite-containing flow yet identified at Mt. Baker. The sample containing pseudobrookite (04-MB-105) was collected from an outcrop adjacent to the Ptarmigan Ridge trail east of Coleman Pinnacle.

ANALYTICAL METHODS AND DATA REDUCTION

Electron microprobe analysis of Fe-Ti oxides was conducted on a four-spectrometer JEOL 733 Superprobe at the University of Washington using a fixed accelerating voltage of 15 kV, a 15 nA current, and a focused beam. Natural and synthetic standards were used for calibration: synthetic rutile (Ti), spinel (Al), synthetic chromite (Cr), Elba hematite (Fe), NiO (Ni), and Nuevo garnet (Mn). Analytical accuracy was monitored through repeat analysis of three natural ilmenites (Sawyer from U. C. Berkeley; A128 and K13-131.8 from A. T. Anderson, U. Chicago), Snetsinger magnetite, and Elba hematite. To minimize overlap, each analysis was located on back scattered electron images of the grain analyzed. Counts were collected at peak positions and at both background positions in all analyses. Data reduction employed the ZAF correction procedures of Armstrong (1988) with first approximation of O in oxide minerals taken by difference from 100% analysis total.

Iron in the Fe-Ti oxides is distributed between ferrous and ferric iron on the basis of the ideal formula for each mineral type, i.e., 3 cations to 5 oxygens for pseudobrookites, 3 cations to 4 oxygens for titanomagnetites and 2 cations to 3 oxygens for ilmenites. In addition to Fe, Ti and O, the oxides contain substantial Mg and lesser Al and Mn. Ilmenite compositions can be expressed in terms of the mole fractions of five end-members: $FeTiO_3$, $MgTiO_3$, Fe_2O_3, $MnTiO_3$ and Al_2O_3. Titanomagnetite compositions can be expressed in terms of nine end-members i.e., titanates of Fe, Mg and Mn; aluminates of Fe, Mg and Mn; and ferrites of Fe^{2+}, Mg and Mn; here

Always consult and cite the final, published document. See http://www.minsocam.org or GeoscienceWorld

we assume that the relative proportions of Fe^{2+}, Mg and Mn are the same in the three series (Evans et al., 2006). Pseudobrookite compositions can be expressed in terms of five end-members: $FeTi_2O_5$, Fe_2TiO_5, $MgTi_2O_5$, $MnTi_2O_5$ and Al_2TiO_5. The corrected analyses are reported in Table 1 along with mole fractions normalized to the three dominant end-members in each mineral group. Analytical errors are summarized in the footnote.

PETROGRAPHY AND CHEMICAL COMPOSITION

Coleman Pinnacle andesite whole-rock samples form a unique compositional trend that plots at higher K_2O values than andesites of the main Mt. Baker fractionation trend (Fig. 2). The composition (and analytical methods) of the pseudobrookite-bearing sample, 04-MB-105, is given in the caption to Fig. 2. The Coleman Pinnacle andesite contains phenocrysts of plagioclase, orthopyroxene, clinopyroxene, and hornblende and microphenocrysts of ilmenite, titanomagnetite and pseudobrookite, apatite and zircon set in a glassy matrix of rhyolitic composition with plagioclase and pyroxene microlites. The andesite also contains glomerophyric clusters of clinopyroxene, orthopyroxene, plagioclase, ilmenite, titanomagnetite and pseudobrookite, apatite and rhyolitic glass. The Coleman Pinnacle flow has the highest hornblende content of all andesite and basalt flows sampled to date at Mt. Baker. Hornblende is a near-liquidus phase, indicating H_2O contents of ~4% in the initial magma (Eggler, 1972).

FE-TI OXIDES

Textural varieties of coexisting Fe-Ti oxides in sample 04-MB-105 are illustrated in Fig. 3 and compositional data for each assemblage are plotted in Fig. 4. The symplectitic intergrowth

Always consult and cite the final, published document. See http://www.minsocam.org or GeoscienceWorld

of pseudobrookite and titanomagnetite (Fig. 3f) is particularly interesting because it shows three coexisting Fe-Ti oxides in intimate contact.

Mg is a major constituent of the pseudobrookites in the Coleman Pinnacle andesite. Grains in the symplectic intergrowth with titanomagnetite (Fig. 3f) are unusually rich in Mg with Mg/Fe^{2+} = 1.5 to 1.7 (molar basis). Grains intergrown with or surrounded by ilmenite (Fig. 3b-e) have lower Mg (molar Mg/Fe^{2+} = 0.7 to 1.1). In addition to the essential components (Ti, Fe, Mg and O), pseudobrookite intergrown with or surrounded by ilmenite has Al_2O_3 contents of ~0.5 wt% while grains intergrown with titanomagnetite contain up to 1.2% wt% Al_2O_3. Cr and Mn are minor constituents.

TEMPERATURE AND REDOX STATE OF COLEMAN PINNACLE LAVAS

The temperatures and oxygen fugacities calculated for two Coleman Pinnacle hornblende andesites (pseudobrookite-bearing 04-MB-105, and pseudobrookite-free 04-MB-101B) are shown in Fig. 5 and are based on the recent recalibration of the Fe-Ti oxide geothermometer–oxybarometer of Ghiorso and Evans (2008). For comparison, data from the coeval Table Mountain pyroxene andesite flow sequence (Fig. 1) at Mt. Baker (309 to 301 ka; Hildreth et al., 2003) are also plotted. The temperature range (900-1000° C) of the Coleman Pinnacle flow is consistent with temperatures of formation given by coexisting orthopyroxene and clinopyroxene (Fig. 3a) in the pseudobrookite-bearing inclusions (~960° C). The pseudobrookite-bearing Coleman Pinnacle sample is the most strongly oxidized with an f_{O2} range of NNO + 1.5 to + 1.75, whereas the pseudobrookite-free sample plots at ~NNO + 1. Table Mountain two-pyroxene andesites, which contain only minor amphibole, formed under more reducing conditions of NNO to NNO + 0.75.

Always consult and cite the final, published document. See http://www.minsocam.org or GeoscienceWorld

DISCUSSION

In the TiO_2–FeO–$FeO_{1.5}$ system, compositions of coexisting pseudobrookite and ilmenite uniquely define temperature and oxygen fugacity. The relevant reactions are:

$$3FeTiO_3\ (ilm) + ½\ O_2 = Fe_2TiO_5\ (psb) + FeTi_2O_5\ (psb) \quad (1)$$

$$2Fe_2TiO_5\ (psb) = 2FeTiO_3\ (ilm) + Fe_2O_3\ (hem) + ½\ O_2 \quad (2)$$

$$FeTiO_3\ (ilm) + Fe_2TiO_5\ (psb) = FeTi_2O_5\ (psb) + Fe_2O_3\ (hem) \quad (3)$$

where ilm = ilmenite, psb = pseudobrookite solid solution, and hem = hematite. The exchange reaction (3) is not independent and is the sum of reactions (1) + (2).

At constant pressure, this system is divariant. Accordingly, specifying the compositions of the two crystalline phases uniquely fixes the temperature and oxygen fugacity. Anovitz et al. (1985) presented a thermodynamic analysis of the equilibria between these two phases and developed a preliminary geothermometer/oxybarometer assuming that pseudobrookites formed ideal solid solutions. As part of an experimental study in the TiO_2–FeO–$FeO_{1.5}$ system aimed at refining the Fe-Ti oxide geothermometer–oxybarometer, Lattard et al. (2005) synthesized coexisting ilmenite–pseudobroookite pairs at 1000, 1100, 1200 and 1300° C at oxygen fugacities ranging from $10^{-3.3}$ to $10^{-12.3}$. In an experimental study on the effect of Mg on phase assemblages in the TiO_2–FeO–$FeO_{1.5}$ system, Speidel (1970) observed in two runs at high Mg contents and high f_{O2} that titanomagnetite + pseudobrookite was the stable assemblage. However, Speidel did not determine the compositions of the pseudobrookite.

The compositions of coexisting ilmenite and pseudobrookite from the Lattard et al. (2005) experiments are plotted on a Roozeboom diagram in Fig. 6. Apart from the data at 1000° C, which is based on only three data points, the distribution coefficient of the exchange reaction

Always consult and cite the final, published document. See http://www.minsocam.org or GeoscienceWorld

(eq. 3) does not appear to have significant temperature dependence. However, the deviation of the experimental data from curves for constant K_D (K_D = 0.6 shown) most likely reflects substantial deviations from ideal mixing for both solid solutions.

The compositions of coexisting pseudobrookite and ilmenite at Mt. Baker are plotted on Fig. 6 and indicate an oxygen fugacity of NNO + 2 to 3, slightly higher than calculated using ilmenite–titanomagnetite pairs from the same sample. However, these oxygen fugacities should, at best, be considered semi-quantitative since the natural pairs crystallized at lower temperatures than the experimental pairs and contain substantial concentrations of MgO.

The occurrence of ***three*** coexisting oxides in the Coleman Pinnacle andesite, apparently forming an equilibrium assemblage (Figs. 3c and f), is extremely rare. The occurrence of abundant rhyolitic glass and glassy melt inclusions in pseudobrookite establish that this is a magmatic crystallization phenomenon. Other examples of rocks containing three oxide phases have been reported (e.g., Anderson and Wright, 1972; Stähle and Koch, 2003) but the textural evidence suggests disequilibrium assemblages. Some of the three-oxide assemblages in the Katzenbuckel syenite (Fig. 5 in Stähle and Koch, 2003) appear similar to those at Coleman Pinnacle, but these are interpreted as primary ilmenite–titanomagnetite pairs in which the ilmenite has been partly replaced by secondary pseudobrookite.

Mass balance calculations presented in Table 2 show that the Coleman Pinnacle three-oxide assemblages cannot be explained as an isochemical breakdown product of the ilmenite. For the assemblage shown in Fig. 3f, combining the measured pseudobrookite and titanomagnetite compositions in relative proportions defined by their areas (53.6% pseudobrookite, 46.4% titanomagnetite; calculated in Adobe Photoshop) generates an ilmenite composition that is ~2.2 wt. % higher in TiO_2 and 3.7 wt. % lower in FeO* than the measured composition. Since

Always consult and cite the final, published document. See http://www.minsocam.org or GeoscienceWorld

206 volumes may differ substantially from areas, we also allowed the proportions of pseudobrookite
207 and titanomagnetite to vary freely until finding a best-fit match to the ilmenite. A combination of
208 47.5% pseudobrookite and 52.5% titanomagnetite generates an ilmenite with appropriate Ti and
209 Fe contents, but has ~1 wt. % more MgO and Al_2O_3 than measured. The involvement of melt
210 could account for the difference, but this would imply a reaction relationship rather than
211 isochemical breakdown, with ilmenite + melt reacting to form pseudobrookite + magnetite,
212 implying equilibrium among all phases.

213 In the TiO_2–FeO–$FeO_{1.5}$ system under isobaric conditions, the three phase assemblage of
214 ilmenite + titanomagnetite + pseudobrookite defines a univariant assemblage. Such an
215 assemblage is theoretically possible, although not observed over the wide range of temperatures
216 and oxygen fugacities studied experimentally in this system. However, the addition of Mg as a
217 major component increases the degrees of freedom of the system, stabilizing the three phase
218 assemblage. The experimental results of Pownceby and Fisher-White (1999) are particularly
219 relevant in this case and provide a rationale for the occurrence of an apparently stable three-
220 phase assemblage. In the following discussion of the Pownceby and Fisher-White (1999) data, it
221 is convenient to adopt their terminology, i.e., spinel (isometric) solid solutions are abbreviated as
222 M_3O_4, ilmenite (rhombohedral) solid solutions as M_2O_3 and pseudobrookite (orthorhombic) solid
223 solutions as M_3O_5, where M = Fe^{2+}, Fe^{3+}, Mg, Ti and minor Mn and Al.

224 Fig. 7 summarizes phase relations in the ternary subsystems of the quaternary TiO_2–
225 MgO–FeO–$FeO_{1.5}$ system at P = 1 bar, T ~900° C, and at log f_{O2} ranging from -0.7 (air) to -17
226 (IW). In the MgO–TiO_2–$FeO_{1.5}$ subsystem (Fig. 7a), experimental data are sparse along the
227 $MgTi_2O_5$–Fe_2TiO_5 join. However, since both end members are stable to relatively low
228 temperatures (Lindsley, 1991), we infer a complete solid solution at 900° C. Between 900° and

Always consult and cite the final, published document. See http://www.minsocam.org or GeoscienceWorld

1200° C, Pownceby and Fisher-White (1999) experimentally located two compositional areas where two distinct three-phase assemblages (M_3O_4–M_2O_3–M_3O_5) are stable, separated by a field where two phases (M_3O_4–M_3O_5) coexist (Fig. 7a). The two-phase field becomes narrower as temperature decreases, and Pownceby and Fisher-White estimated that the $M_3O_4 + M_3O_5$ assemblage is not stable at T < 800° C. Two structurally distinct solid solutions (α-M_2O_3 and α'-M_2O_3) define the immiscibility gap along the geikielite–hematite join.

In the TiO_2–MgO–FeO subsystem (Fig. 7b) between 900° and 1140° C, stable assemblages are (1) $M_3O_4 + M_2O_3$, (2) $M_2O_3 + M_3O_5$, (3) $M_2O_3 + M_3O_5$ + rutile, (4) M_2O_3 + rutile and (5) M_3O_5 + rutile. The solid solution between $MgTi_2O_5$ and $FeTi_2O_5$ is complete at T > 1140° C (Lindsley et al., 1974) but at lower temperatures, $FeTi_2O_5$ breaks down to rutile + ilmenite and the M_3O_5 solid solution becomes increasingly restricted to more magnesian compositions (Fig. 7b). The two phase assemblage $M_3O_4 + M_3O_5$ is **not** stable in this subsystem.

Phase relations in the TiO_2–FeO–$FeO_{1.5}$ system (Fig. 7c) are summarized by Lindsley (1991) and recently extended to higher f_{O2} conditions by Lattard et al. (2005), Evans et al. (2006) and Ghiorso and Evans (2008). The tie lines shown in Fig. 7c are based on Lindsley (1991) and Fig. 14 in Ghiorso and Evans (2008) for T = 900°C and f_{O2} ~NNO - 2 to NNO + 2. In summary, there is no evidence of a stable $M_3O_4 + M_3O_5$ assemblage in this subsystem over the wide range of temperatures and redox states studied experimentally. However, the presence of an immiscibility gap in the ilmenite–hematite solid solution series is clearly indicated by experiments (Burton, 1984) and the occurrence of {0001} hematite lamellae in an ilmenite host in plutonic and metamorphic samples (Haggerty, 1991a). In volcanic rocks, the exsolution, if present, is not visible optically or in BSE/SE images and host–lamellae intergrowths are not resolvable in microprobe analysis.

Always consult and cite the final, published document. See http://www.minsocam.org or GeoscienceWorld

In the quaternary system, with decreasing oxygen fugacity and decreasing Mg/(Mg+Fe^{2+}), the two- and three-phase regions shown in Fig. 7a extend into the tetrahedron (e.g., see Fig. 8d in Haggerty, 1991b). On the basis of phase compositions observed in coexisting Fe-Ti oxides in the Coleman Pinnacle andesite (Table 1), we postulate that, at an intermediate Mg/(Mg+Fe^{2+}) value of ~0.6, there is a tie line flip and the M_3O_4–M_3O_5 tie line is replaced by the α-M_2O_3–α'M_2O_3 tie line. This sequence is illustrated in Fig. 8. It is worth noting that the assemblage with the most compelling evidence for an equilibrium M_3O_4–M_3O_5 pair (Fig. 3f) has the highest Mg/(Mg+Fe^{2+}) values in both the spinel and pseudobrookite solid solutions. In the syenite dike at Katzenbuckel volcano, the three-oxide assemblage previously interpreted as disequilibrium may in fact represent an equilibrium assemblage stabilized by Mg, as the pseudobrookites contain 4.2-5.6 wt. % MgO (Stähle and Koch, 2003), a range similar to that at Coleman Pinnacle.

As with Mg, the addition of Al to the TiO_2–FeO–$FeO_{1.5}$ system has also been shown experimentally to stabilize the three Fe-Ti oxide assemblage (Sauerzapf, 2006). The Al_2O_3 contents of the Coleman Pinnacle pseudobrookites are substantially lower (0.5 to 1.1 wt. %) than those of the synthesized pseudobrookites (2.9 to 4.6 wt. %), too low to account for the presence of titanomagnetite. However, there is a positive correlation between Mg and Al in the Coleman Pinnacle pseudobrookites, indicating that Al may have played a minor role in stabilizing the assemblage.

Elevated Mg/(Mg+Fe^{2+}) in the Coleman Pinnacle Fe-Ti oxides is most likely a consequence of the high f_{O2} of the magma. With an oxygen fugacity range of NNO + 1.5 to NNO + 1.75, corresponding to $Fe^{3+}/\Sigma Fe = 0.43$ (using the equation of Kress and Carmichael, 1991), the pseudobrookite-bearing Coleman Pinnacle magma is among the most oxidized on record

Always consult and cite the final, published document. See http://www.minsocam.org or GeoscienceWorld

(e.g., Evans et al., 2012). As discussed above, other pseudobrookite + titanomagnetite assemblages occur in magmatic systems that also have high oxygen fugacities and high Mg in Fe-Ti oxides (where data are available). Rapid quenching of the Coleman Pinnacle magma from relatively high temperatures, as evidenced by the presence of glass and temperatures of 900-1000° C, preserved the coexisting pseudobrookite + titanomagnetite assemblage relative to ilmenite + titanomagnetite or ilmenite + pseudobrookite.

In addition to having the highest f_{O2} at Mt. Baker, the Coleman Pinnacle flow also has the highest water content, providing another example of a magma in which redox state correlates with water content (e.g., Kelley and Cottrell, 2009). The Coleman Pinnacle andesite also has the highest abundances of fluid-mobile elements measured in Mt. Baker lavas (E. Mullen, unpublished data), a feature consistent with high H_2O and generally attributed to slab-derived fluid input to the mantle wedge (Pearce and Peate, 1995). Although it is beyond the scope of this paper to discuss in detail the origin of the oxidized nature of the Coleman Pinnacle magma, the presence of Fe^{3+}-rich cores in amphibole phenocrysts ($Fe^{3+}/\Sigma Fe$ up to 0.8) (Mullen and McCallum, 2006) is consistent with a primary magmatic signature. As the Mt. Baker basalts have redox states approximately equivalent to the NNO buffer (Mullen and McCallum, in review), crustal processes may have increased the f_{O2} of the Coleman Pinnacle magma. However, Pb isotope ratios indicate minimal crustal input (Mullen, 2011), indicating that the high f_{O2} may have been inherited from the mantle source.

ACKNOWLEDGMENTS

This work was supported by funds provided to the first author from a National Science Foundation Graduate Research Fellowship, a University of Washington NASA Space Grant

Always consult and cite the final, published document. See http://www.minsocam.org or GeoscienceWorld

Fellowship, several fellowships (Peter Misch, David A. Johnston, Wernicke Livingston) and graduate research fund awards from the Department of Earth and Space Sciences at the University of Washington. We thank Bernard Evans for many stimulating discussions on Fe-Ti oxide problems and for reviewing an early version of this paper. We are grateful to Dominique Lattard and Malcolm Rutherford for providing detailed and insightful reviews that markedly improved the manuscript.

REFERENCES

Anderson, A.T., Bunch, T.E., Cameron, E.N., Haggerty, S.E., Boyd, F.R., Finger, L.W., James, O.B., Keil, K., Prinz, M., Ramdohr, P. and El Goresy, A. (1970) Armalcolite: A new mineral from the Apollo 11 samples. Proceeding of the Apollo 11 Lunar Science Conference, Geochimica et Cosmochimica Acta, Supplement 1, 55-64.

Anderson, A.T., and Wright, T.L. (1972) Phenocryst and glass inclusions and their bearing on oxidation and mixing of basaltic magmas, Kilauea Volcano, Hawaii. American Mineralogist, 57, 188-216.

Anovitz, L.M., Treiman, A.H., Essene, E.J., Hemingway, B.S., Westrum, E.F.Jr., Wall, V.J., Burriel, R, and Bohlen, S.R. (1985) The heat capacity of ilmenite and phase equilibria in the system Fe-Ti-O. Geochimica et Cosmochimica Acta, 49, 2027-2040.

Armstrong, J.T. (1988) Quantitative analysis of silicate and oxide minerals: comparison of Monte Carlo, ZAF, and □(ρz) procedures. In: Newbury, D.E. (Ed.), *Microbeam Analysis – 1988*. San Francisco Press, San Francisco, CA, pp. 239–246.

Bowles, J.F.W. (1988) Definition and range of composition of naturally occurring minerals with the pseudobrookite structure. American Mineralogist, 73, 1377-1383.

Always consult and cite the final, published document. See http://www.minsocam.org or GeoscienceWorld

Buddington, A.F., and Lindsley, D.H. (1964) Iron-titanium oxide minerals and synthetic equivalents. Journal of Petrology, 5, 310-357.

Burton, B.P. (1984) Thermodynamic analysis of the system Fe_2O_3-$FeTiO_3$. Physics and Chemistry of Minerals, 11, 132-139.

Eggler, D.H. (1972) Amphibole stability in H_2O-undersaturated calc-alkaline melts. Earth and Planetary Science Letters, 15, 28-34.

Evans, B.W., Scaillet, B., and Kuehner, S.M. (2006) Experimental determination of co-existing iron-titanium oxides in the systems FeTiAlO, FeTiAlMgO, FeTiAlMnO, and FeTiAlMgMnO at 800 and 900° C, 1–4 kbar, and relatively high oxygen fugacity. Contributions to Mineralogy and Petrology, 152, 149–167.

Evans, K.A., Elburg, M.A., and Kamenetsky, V.S. (2012) Oxidation state of subarc mantle. Geology, 40, 783-786.

Ghiorso, M.S., and Evans, B.W. (2008) Thermodynamics of rhombohedral oxide solid solutions and a revision of the P-T two-oxide geothermometer and oxygen-barometer. American Journal of Science, 308, 957-1039.

Haggerty, S.E. (1991a) Oxide textures—a mini-atlas. In: Lindsley, D.H. (ed) Oxide minerals: petrologic and magnetite significance, Reviews in Mineralogy, vol 25. Mineralogical Society of America, Washington, pp 129–137.

Haggerty, S.E. (1991b) Oxide mineralogy of the upper mantle. In: Lindsley, D.H. (ed) Oxide minerals: petrologic and magnetic significance, Reviews in Mineralogy, vol 25. Mineralogical Society of America, Washington, pp 355–416.

Always consult and cite the final, published document. See http://www.minsocam.org or GeoscienceWorld

Hildreth, W., Fierstein, J., and Lanphere, M.A. (2003) Eruptive history and geochronology of the Mount Baker volcanic field, Washington. Geological Society of America Bulletin, 115, 729-764.

Johnston, A.D., and Stout, J.H. (1984) A highly oxidized ferrian salite-, kennedyite-, forsterite- and rhonite-bearing alkali gabbro from Kauai, Hawaii, and its mantle xenoliths. American Mineralogist, 69, 57-68.

Kelley, K.A, and Cottrell, E. (2009) Water and the oxidation state of subduction zone magmas. Science, 325, 605-607.

Kress, V.C., and Carmichael, I.S.E (1991) The compressibility of silicate liquids containing Fe_2O_3 and the effect of composition, temperature, oxygen fugacity and pressure on their redox states. Contributions to Mineralogy and Petrology, 108, 82-92.

Lattard, D., Sauerzapf, U., and Martin K. (2005) New calibration data for the Fe–Ti oxide thermo-oxybarometers from experiments in the Fe–Ti–O system at 1 bar, 1,000–1300°C and a large range of oxygen fugacities. Contributions to Mineralogy and Petrology, 149, 735–754.

Le Roex, A.P. (1985) Geochemistry, mineralogy and magmatic evolution of basaltic and trachytic lavas from Gough Island, South Atlantic. Journal of Petrology, 26, 149-186.

Lindsley, D.H. (1991) Experimental studies of oxide minerals. In: Lindsley, D.H. (ed.) Oxide minerals: petrologic and magnetic significance, Reviews in Mineralogy. Mineralogical Society of America, Washington, 25, pp 69-100.

Lindsley, D.H., Kesson, S.E., Hartzman, M.J., and Cushman, M.K. (1974) The stability of armalcolite: experimental studies in the system MgO-Fe-Ti-O. Geochimica et Cosmochimica Acta Supplement 5, 1, 521-534.

Always consult and cite the final, published document. See http://www.minsocam.org or GeoscienceWorld

Mullen, E.K. (2011) Petrology and geochemistry of the Mount Baker volcanic field: constraints on source regions and terrane boundaries, and comparison with other Cascade Arc volcanic centers. Ph.D. dissertation, University of Washington, 388p.

Mullen, E.K., and McCallum, I.S. (2006) Amphiboles as indicators of redox states in volcanic rocks. EOS Transactions AGU, 87(52), Fall Meeting Supplement, Abstract V51B-1678.

Pearce, J.A., and Peate, D.W. (1995) Tectonic implications of the composition of volcanic arc magmas. Annual Reviews in Earth and Planetary Science, 23, 251-285.

Pownceby, M.I., and Fisher-White, M.J. (1999) Phase equilibria in the systems Fe_2O_3-MgO-TiO_2 and FeO-MgO-TiO_2 between 1173 and 1473°K, and Fe^{2+}-Mg mixing properties of ilmenite, ferrous-pseudobrookite and ulvöspinel solid solutions. Contributions to Mineralogy and Petrology, 135, 198-211.

Sauerzapf, U. (2006) New experimental data for a re-calibration of the Fe-Ti oxide thermo-oxybarometers. Ph.D. dissertation, Heidelberg: Ruprecht-Karls-Universität, 231p.

Speidel, D.H. (1970) Effect of magnesium on the iron-titanium oxides. American Journal of Science, 268, 341-353.

Stähle, V., and Koch, M. (2003) Primary and secondary pseudobrookite minerals in volcanic rocks from the Katzenbuckel Alkaline Complex, southwestern Germany. Schweizerische Mineralogische and Petrographische Mitteilungen, 83, 145-158.

Tabor, R.W., Haugerud, R.A., Hildreth, W., and Brown, E.H. (2003) Geologic map of the Mount Baker 30 x 60 minute quadrangle, Washington. U. S. Geological Survey Map I-2660, scale 1:100,000.

Tucker, D.S. (2006) Cross section through the Hannegan Caldera. Geological Society of America Digital Map and Chart Series 3, 2 sheets, scale: 1:24,000.

Always consult and cite the final, published document. See http://www.minsocam.org or GeoscienceWorld

388 van Kooten, G.K. (1980) Mineralogy, petrology and geochemistry of an ultrapotassic basaltic
389 suite, Central Sierra Nevada, California, USA. Journal of Petrology, 21, 651-684.
390
391
392

Always consult and cite the final, published document. See http://www.minsocam.org or GeoscienceWorld

FIGURE CAPTIONS

Figure 1. (a) Geologic map of the Mt. Baker volcanic field, after Hildreth et al. (2003), Tabor et al. (2003), and Tucker (2006). The Coleman Pinnacle flow is shown in black, the Table Mountain flow with a stippled pattern, and other volcanic rocks in light gray. Plutonic rocks are shown with a (+) pattern. Elevation contours (gray dotted lines) are given in feet. (b) Photograph of Coleman Pinnacle with Mt. Baker stratocone in the background.

Figure 2. K_2O vs. SiO_2 for Mount Baker volcanic field. Analyses are from Hildreth et al. (2003) and Mullen (2011). Coleman Pinnacle samples are shown by black circles. All other analyses are shown as small gray circles. Pseudobrookite-bearing andesite 04-MB-105 from Coleman Pinnacle is shown by the star. Composition of 04-MB-105 (wt.%): SiO_2: 59.2, TiO_2: 1.00, Al_2O_3: 16.7, FeO*: 5.40, MnO: 0.10, MgO: 2.84, CaO: 6.03, Na_2O: 4.81, K_2O: 2.93, P_2O_5: 0.43 (un-normalized; all iron reported as FeO). Whole data obtained by X-ray fluorescence spectrometry (XRF) at the Washington State University GeoAnalytical Laboratory. Samples were crushed by hardened steel jaw crusher and pulverized by agate ball mill. XRF methods, accuracy, and precision are described at http://www.sees.wsu.edu/Geolab/note/xrf.html. Uncertainties on major element oxides are <2% relative except for K_2O (~3-7%).

Figure 3. Backscattered electron images (false color) showing the variety of occurrences of titanomagnetite, ilmenite and pseudobrookite in sample 04-MB-105. Each assemblage is assigned a number, given in square brackets, that corresponds to compositions listed in Table 1. Individual pseudobrookites are also assigned numbers, given in parentheses, which are used to identify data

Always consult and cite the final, published document. See http://www.minsocam.org or GeoscienceWorld

points in Fig. 4 and Table 1. Abbreviations on images: opx: orthopyroxene, cpx: clinopyroxene, ap: apatite, plag: plagioclase, mag: titanomagnetite, ilm: ilmenite, psb: pseudobrookite, glass: K-Na-Al-Si-rich rhyolitic glass, zrn: zircon. (a) glomerophyric cluster of orthopyroxene, clinopyroxene, Fe-Ti oxides, apatite and zircon in a vesicular matrix of rhyolitic glass with plagioclase laths. Areas enclosed in white boxes are enlarged in (b) and (c). (b) Subskeletal pseudobrookite (psb3) intergrown with ilmenite [3]. Note the rhyolite melt inclusion (labeled as glass). (c) Wedge-shaped pseudobrookite (psb2) surrounded by ilmenite adjacent to equant titanomagnetite, all embedded in glass [2]. (d) Symplectite of ilmenite and pseudobrookite (psb6) [6]. Large black arrow marks the melt inclusion at right center. (e) Intergrowth of skeletal pseudobrookite (psb4) and ilmenite [4]. Note the partial rim of titanomagnetite around ilmenite. (f) Ilmenite core surrounded by a symplectite of titanomagnetite and pseudobrookite (psb1) [1].

Figure 4. Coexisting pseudobrookite, ilmenite, and titanomagnetite from Coleman Pinnacle andesite projected (a) from respective Mg end-members on to binary joins in TiO_2-FeO-$FeO_{1.5}$ plane and (b) from respective Fe^{2+} end-members on to binary joins in the TiO_2-MgO-$FeO_{1.5}$ plane. The legend correlates with the images in Fig. 3. Tie lines are drawn between coexisting minerals. Dashed tie lines indicate pairs that might not be in equilibrium (psb2–mag and psb4–mag; illustrated in Fig. 3). Abbreviations: Fpb: "ferropseudobrookite" ($FeTi_2O_5$), Kar: "karrooite" ($MgTi_2O_5$), Psb: pseudobrookite (Fe_2TiO_5), Ilm: ilmenite, Hem: hematite, Gk: geikielite, Usp: ulvöspinel, Mag: magnetite, Mfr: magnesioferrite, Qnd: qandilite.

Figure 5. f_{O2} vs. temperature plot for two samples of the Coleman Pinnacle flow (04-MB-105 and 04-MB-101b) and two samples from the coeval Table Mountain flow sequence (04-

Always consult and cite the final, published document. See http://www.minsocam.org or GeoscienceWorld

439 MB-22 and MB4-JV) determined from compositions of coexisting titanomagnetite and ilmenite
440 (Mullen, 2011) using the calibration of Ghiorso and Evans (2008). Buffer curves are shown for
441 NNO, NNO + 1 and NNO + 1.5. Sample 04-MB-105, the most strongly oxidized sample,
442 contains pseudobrookite.
443
444 **Figure 6.** Roozeboom plot of coexisting ilmenite and pseudobrookite from experiments
445 by Lattard et al. (2005) at 1 bar, T = 1000°, 1100°, 1200° and 1300° C in the Fe-Ti-O system.
446 Abbreviations: ilm = ilmenite, fpb = ferropseudobrookite. Mole fractions as reported in Lattard
447 et al. Numbers adjacent to data indicate f_{O2} values (relative to the NNO buffer) for selected
448 experiments at 1200° C. Data for six pairs from the Coleman Pinnacle andesite are plotted as
449 black filled circles. Mole fractions for both X_{ilm} and X_{fpb} were calculated as $Fe^{2+}/(Fe^{2+} +$
450 $0.5*Fe^{3+}$) (in cations). A $K_D = 0.6$ line is shown for reference, where K_D is the distribution
451 coefficient for reaction 3 in the text. Deviations from a symmetrical distribution reflect
452 deviations from ideal mixing for both solid solution series.
453
454 **Figure 7.** Phase relations in the bounding ternary systems in the TiO_2-MgO-FeO-$FeO_{1.5}$
455 system at P=1 bar, T ~900° C and variable f_{O2}. Shaded gray areas represent stable 3-phase
456 assemblages. (a) TiO_2-MgO-$FeO_{1.5}$ subsystem at $f_{O2} = 0.2$ (air) after Fig. 2d in Pownceby and
457 Fisher-White (1999). The M_2O_5 series shows complete solid solution at 900° C. Note the
458 stability of two distinct spinel (M_3O_4) – pseudobrookite (M_3O_5) – ilmenite (M_2O_3) assemblages
459 separated by a stable M_3O_5–M_3O_4 assemblage and the immiscibility gap in the M_2O_3 series. (b)
460 TiO_2–MgO–FeO (f_{O2} ~ IW) subsystem after Lindsley et al. (1974), Lindsley (1991), and
461 Pownceby and Fisher-White (1999). At T <1140° C, $FeTi_2O_5$ ("ferropseudobrookite") breaks

Always consult and cite the final, published document. See http://www.minsocam.org or GeoscienceWorld

462 down to ilmenite + rutile. The $(Mg,Fe)TiO_3$ series and the $(Mg,Fe)_2TiO_4$ series show complete
463 solid solution to temperatures <900° C. (c) TiO_2–FeO–$FeO_{1.5}$ subsystem (f_{O2} ~NNO+2 to NNO-
464 2). M_3O_4–M_2O_3 equilibrium tie lines are based on experimental data (Lindsley, 1991; Lattard et
465 al., 2005; Evans et al., 2006) and the thermodynamic analysis of Ghiorso and Evans (2008)
466 summarized in their Fig. 14. Note the immiscibility gap in the M_2O_3 compositions at 900°C.
467 M_2O_3–M_3O_5 equilibria are based on experiments by Lattard et al. (2005) summarized in Fig. 6.
468
469 **Figure 8**. Schematic representation of stable assemblages in the TiO_2–MgO–FeO–$FeO_{1.5}$
470 system at T ~900-1000° C and variable f_{O2} and Mg/(Mg+Fe), based on the phase relations shown
471 in Fig. 7. (a) High $Fe^{2+}/\Sigma Fe$ systems (Mg-poor, with $Mg/[Fe^{2+}+Mg]$ <0.6) showing the
472 "common" situation involving coexisting titanomagnetite and ilmenite and the less common
473 coexisting ilmenite and pseudobrookite. In volcanic rocks, the exsolved ilmenite is
474 submicroscopic. (b) Intermediate ($Mg/[Mg+Fe^{2+}]$ ~0.6) systems showing a tie line flip. (c) High
475 $Fe^{3+}/\Sigma Fe$ systems (Mg-rich, with $Mg/[Mg+Fe^{2+}]$ >0.6) showing the "rare" situation involving a
476 stable tie line between titanomagnetite and pseudobrookite.
477

Always consult and cite the final, published document. See http://www.minsocam.org or GeoscienceWorld

478 Table 1. Compositions of Fe-Ti oxides (wt. %).

Assemblage	1			2			4			3		5		6	
	Ilm	Psb1	Mag	Ilm	Psb2	Mag	Ilm	Psb4	Mag	Ilm	Psb3	Ilm	Psb5	Ilm	Psb6
wt.%	n=11	n=12	n=15	n=11	n=7	n=9	n=2	n=2	n=2	n=1	n=1	n=1	n=1	n=1	n=2
TiO_2	29.9	53.3	7.56	29.8	52.9	7.84	29.6	52.3	6.96	31.5	53.6	30.6	52.0	29.1	51.7
Al_2O_3	0.46	1.08	2.47	0.36	0.48	1.57	0.40	0.71	1.80	0.36	0.59	0.34	0.67	0.30	0.20
Cr_2O_3	0.02	0.02	0.03	0.03	0.01	0.10	0.02	0.00	0.04	0.02	0.04	0.01	0.02	0.00	0.02
Fe_2O_3	44.7	32.7	53.5	43.7	32.3	52.6	44.7	33.4	54.6	41.6	31.7	42.2	32.2	43.9	33.6
FeO	20.0	6.21	30.4	21.6	8.68	32.4	20.70	7.51	31.02	22.11	7.87	21.11	7.18	21.73	8.72
MnO	0.18	0.09	0.40	0.33	0.19	0.72	0.39	0.21	0.87	0.59	0.29	0.71	0.38	0.38	0.22
NiO	0.01	0.01	0.02	0.02	0.01	0.02	0.00	0.00	0.00	0.01	0.00	0.00	0.00	0.01	0.01
MgO	3.79	5.55	4.84	2.70	4.18	3.27	3.12	4.52	3.62	3.15	4.83	3.16	4.66	2.28	3.73
Total	99.0	98.9	99.2	98.6	98.7	98.5	98.9	98.7	98.9	99.4	99.0	98.1	97.1	97.8	98.1
moles															
Ti	0.57	1.51	0.21	0.57	1.52	0.22	0.57	1.50	0.20	0.60	1.53	0.59	1.51	0.57	1.51
Al	0.01	0.05	0.11	0.01	0.02	0.07	0.01	0.03	0.08	0.01	0.03	0.01	0.03	0.01	0.01
Cr	0.00	0.00	0.00	0.00	0.00	0.00	0.00	0.00	0.00	0.00	0.00	0.00	0.00	0.00	0.00
Fe^{3+}	0.85	0.93	1.48	0.84	0.93	1.49	0.86	0.96	1.53	0.79	0.91	0.81	0.94	0.86	0.98
Fe^{2+}	0.42	0.20	0.93	0.46	0.28	1.02	0.44	0.24	0.97	0.47	0.25	0.45	0.23	0.47	0.28
Mn	0.00	0.00	0.01	0.01	0.01	0.02	0.01	0.01	0.03	0.01	0.01	0.02	0.01	0.01	0.01
Ni	0.00	0.00	0.00	0.00	0.00	0.00	0.00	0.00	0.00	0.00	0.00	0.00	0.00	0.00	0.00
Mg	0.14	0.31	0.27	0.10	0.24	0.18	0.12	0.26	0.20	0.12	0.27	0.12	0.27	0.09	0.22
Cation Sum	2	3	3	2	3	3	2	3	3	2	3	2	3	2	3
O	3	5	4	3	5	4	3	5	4	3	5	3	5	3	5
end members (mole fr.)															
Ilm	0.43			0.47			0.45			0.48		0.46		0.48	

Gk	0.14			0.10			0.12			0.12			0.12			0.09		
Hem	0.43			0.43			0.43			0.40			0.42			0.43		
Fpb		0.20			0.28			0.25			0.256			0.25			0.28	
Kar		0.32			0.24			0.26			0.280			0.26			0.22	
Psb		0.48			0.47			0.49			0.464			0.49			0.50	
Usp			0.22			0.22			0.20									
Mag			0.72			0.74			0.76									
Qnd			0.06			0.04			0.04									

Notes: n = number of data points averaged for each analysis. Average relative errors for EPMA based on counting statistics: 0.59% (Fe), 0.67% (Ti), 1.43% (Mg), 3.07% (Al), 10.7% (Mn), 58.8% (Cr), 94.2% (Ni). Redistribution of iron between Fe^{3+} and Fe^{2+} is based on ideal stoichiometry for each mineral group (described in the text). The three dominant end-member mole fractions are reported for each mineral group, normalized to 1. End-member abbreviations: Ilm = ilmenite, Gk = geikielite, Hem = hematite, Fpb = "ferropseudobrookite", Kar = "karooite", Psb = pseudobrookite (Fe_2TiO_5), Usp = ulvöspinel, Mag = magnetite, Qnd = qandilite.

Table 2. Mass balance calculations for Assemblage 1.

wt%	Measured Ilm	Hypothetical Ilm #1			Hypothetical Ilm #2	
TiO_2	29.8	32.0			29.2	
Al_2O_3	0.36	0.99			1.05	
Cr_2O_3	0.03	0.05			0.06	
Fe_2O_3	43.7	41.7			43.0	
FeO	21.6	19. 7			21.1	
MnO	0.33	0.44			0.47	
NiO	0.02	0.01			0.02	
MgO	2.7	3.76			3.70	
Total	98.6	98.6			98.6	
		Ilm	Psb	Mag	Psb	Mag
	% of image:	5.9	14.3	12.4	-	-
	Normalized %:	-	53.6	46.4	47.5	52.5

Notes: Abbreviations are the same as in Table 1. The composition of hypothetical ilmenite #1 was calculated using the measured compositions of titanomagnetite and pseudobrookite in Assemblage 1 (from Table 1) in relative proportions (listed below the composition) that were determined from their areas in the image in Fig. 3f. The composition of hypothetical ilmenite #2 was calculated using proportions of titanomagnetite and pseudobrookite determined from least-squares calculations to give a best fit match to the measured ilmenite composition. The best fit proportions are listed below the composition.

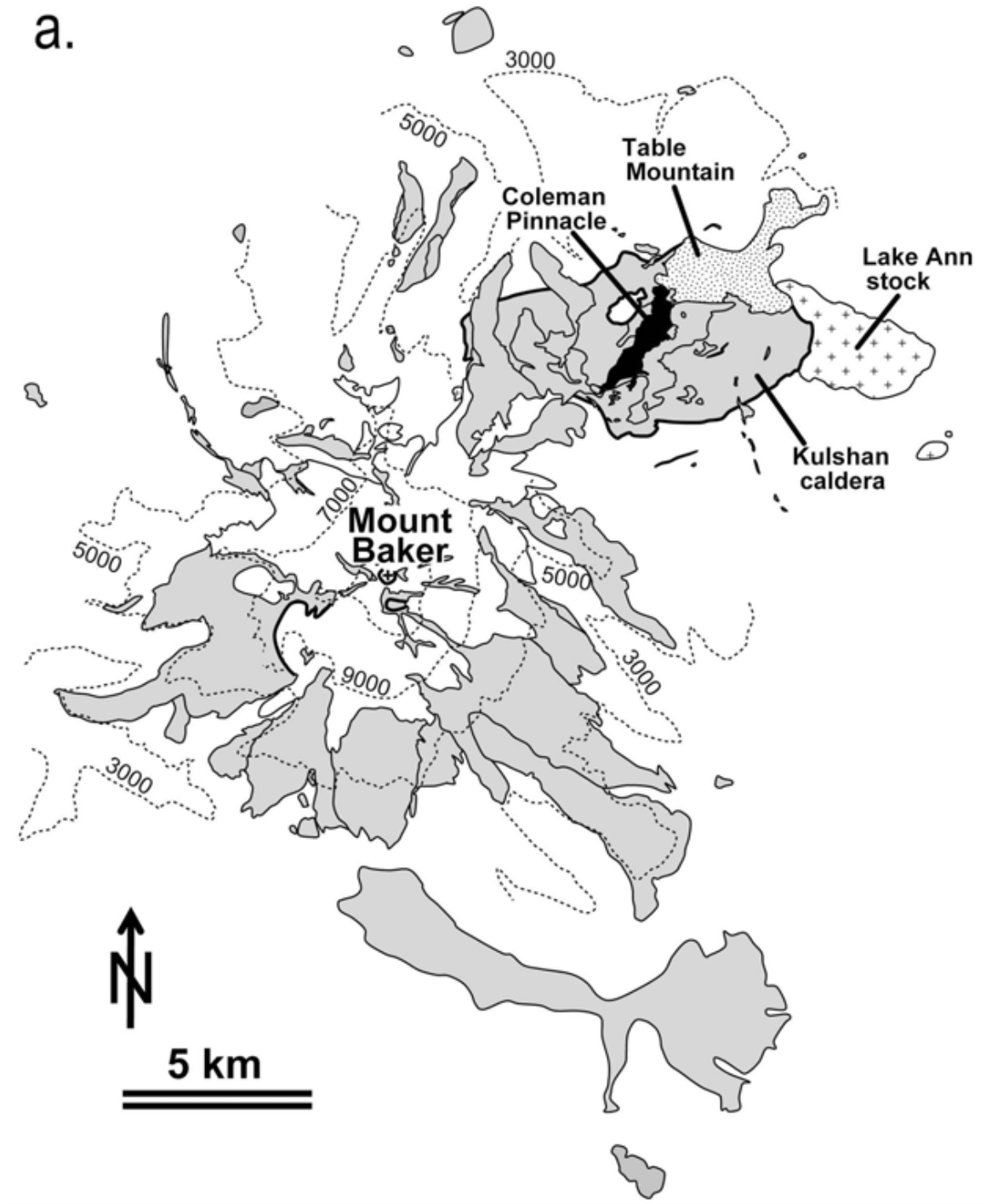
a.
3000
5000
Table
Mountain
Coleman
Pinnacle
Lake Ann
stock
Kulshan
caldera
7000
Mount
Baker
5000
5000
3000
9000
3000
N
5 km

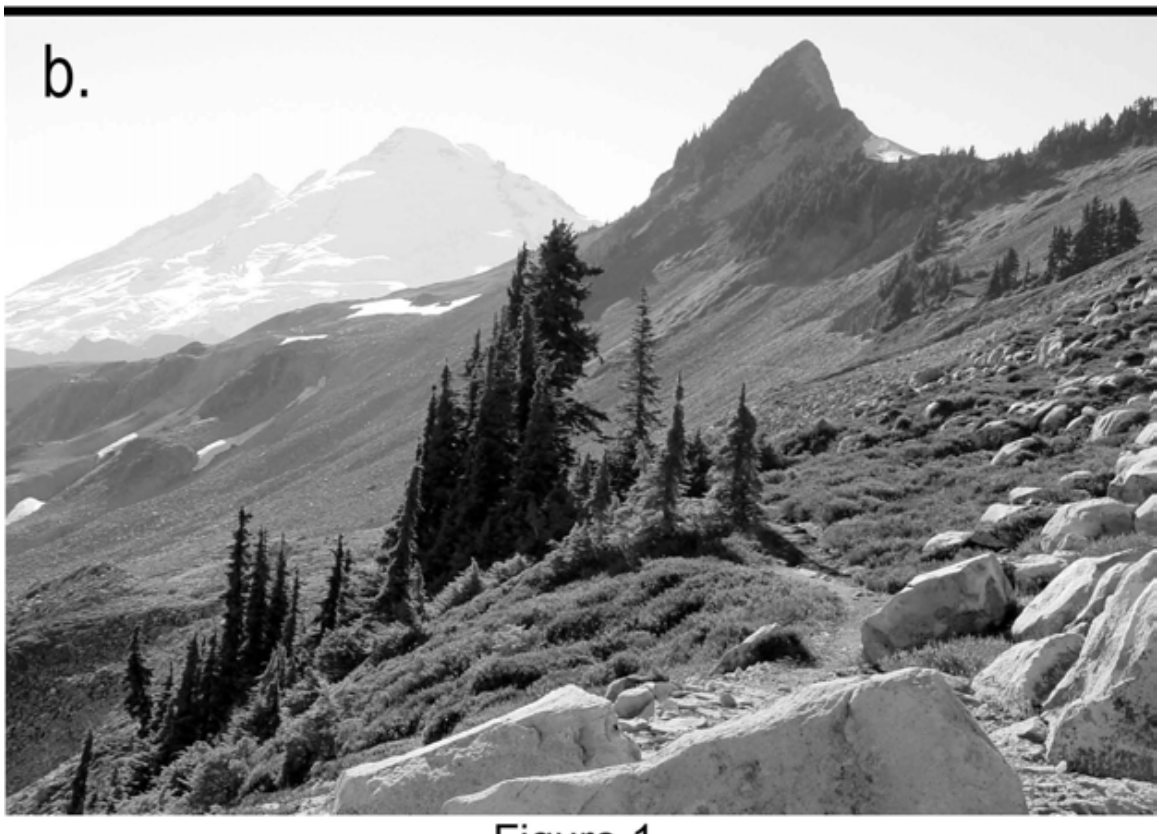
b.

Figure 1

Figure 2

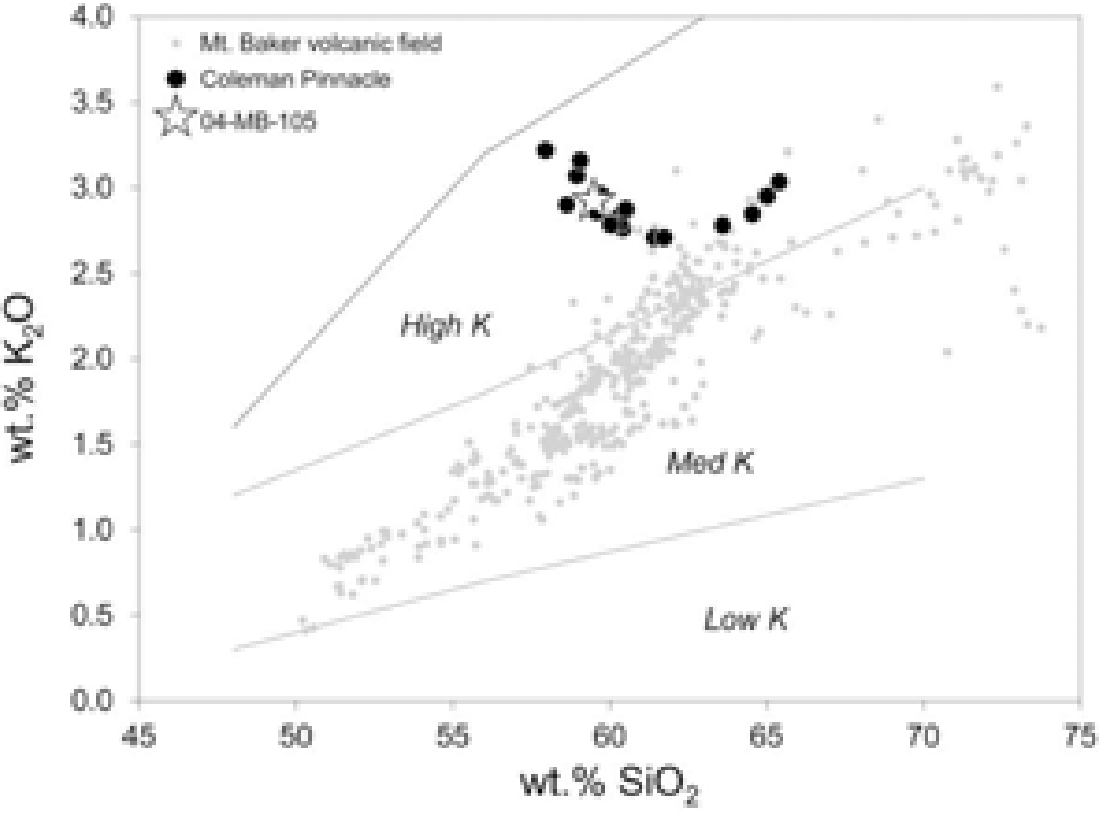
Mt. Baker volcanic field
Coleman Pinnacle
04-MB-105
High K
Med K
Low K
wt.% K2O
wt.% SiO2
4.0
3.5
3.0
2.5
2.0
1.5
1.0
0.5
0.0
45
50
55
60
65
70
75

Figure 3

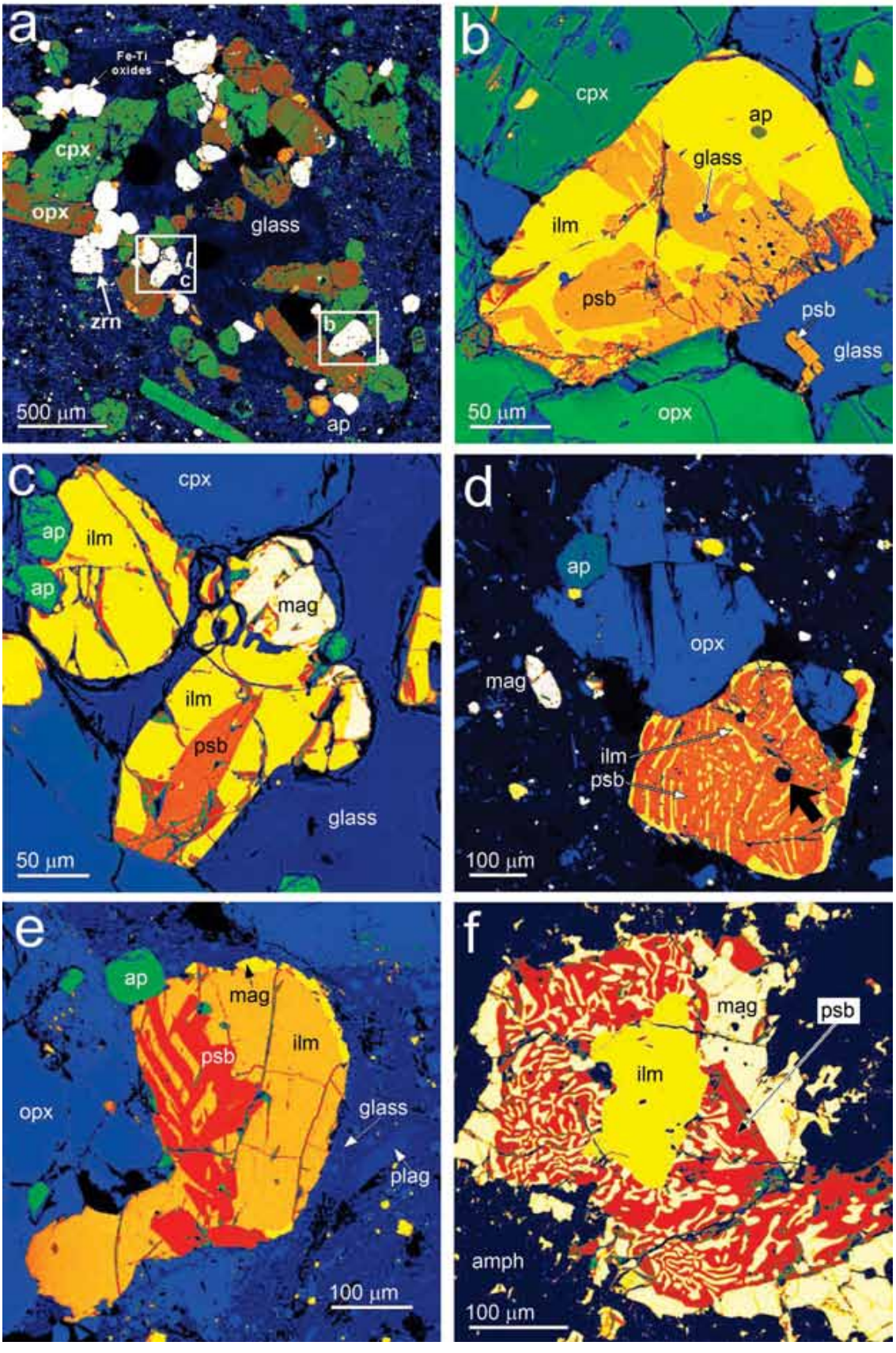
a
Fe-Ti oxides
cpx
opx
glass
c
zrn
b
500 μm
ap
b
cpx
ap
glass
ilm
psb
psb
glass
50 μm
opx
c
cpx
ap
ilm
ap
mag
ilm
psb
glass
50 μm
d
ap
opx
mag
ilm
psb
100 μm
e
ap
mag
psb
ilm
opx
glass
plag
100 μm
f
mag
psb
ilm
amph
100 μm

Figure 4

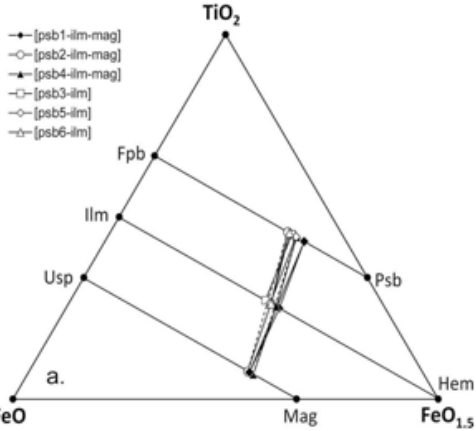
TiO2
[psb1-ilm-mag]
[psb2-ilm-mag]
[psb4-ilm-mag]
[psb3-ilm]
[psb5-ilm]
[psb6-ilm]
Fpb
Ilm
Usp
Psb
a.
Hem
FeO
Mag
FeO1.5

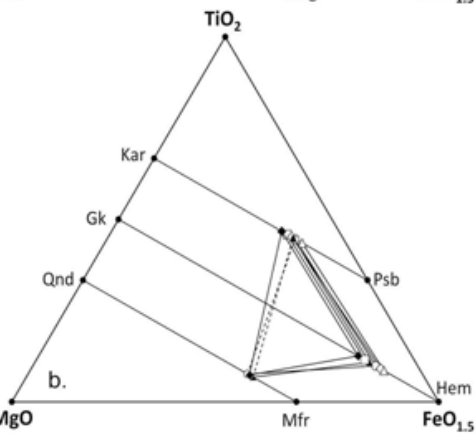
TiO2
Kar
Gk
Qnd
Psb
b.
Hem
MgO
Mfr
FeO1.5

Figure 5

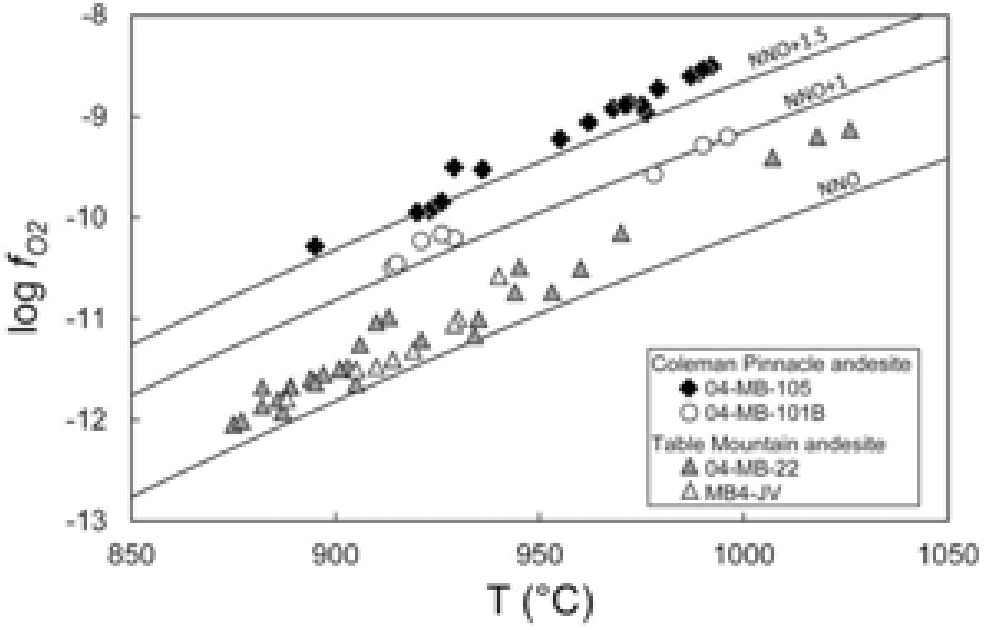
-8
-9
-10
-11
-12
-13
log f_{O2}
850
900
950
1000
1050
T (°C)
NNO+1.5
NNO+1
NNO
Coleman Pinnacle andesite
04-MB-105
04-MB-101B
Table Mountain andesite
04-MB-22
MB4-JV

Figure 6

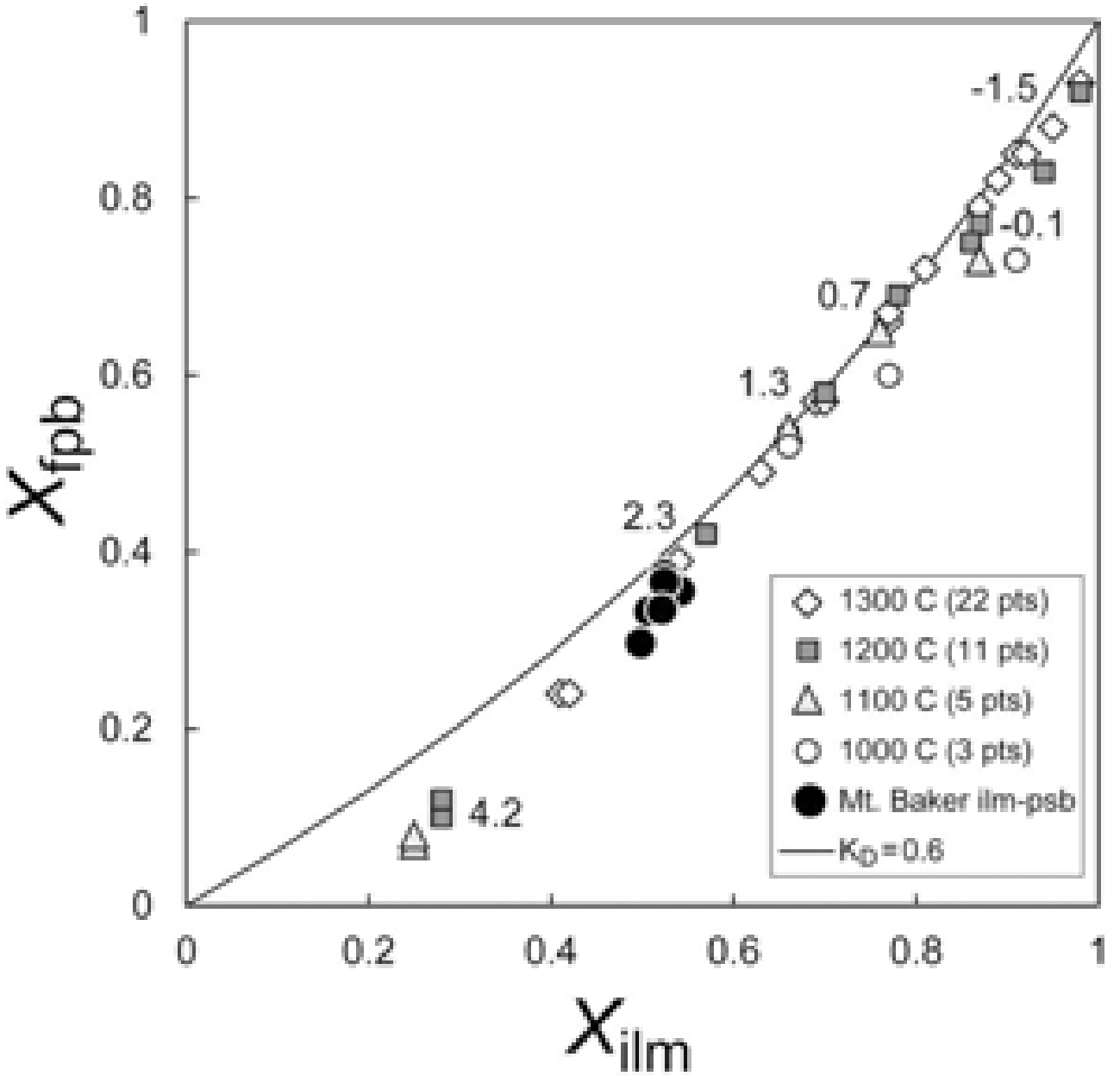
1
0.8
0.6
0.4
0.2
0
0
0.2
0.4
0.6
0.8
1
X_{fpb}
X_{ilm}
-1.5
-0.1
0.7
1.3
2.3
4.2
1300 C (22 pts)
1200 C (11 pts)
1100 C (5 pts)
1000 C (3 pts)
Mt. Baker ilm-psb
$K_D = 0.6$

Figure 7

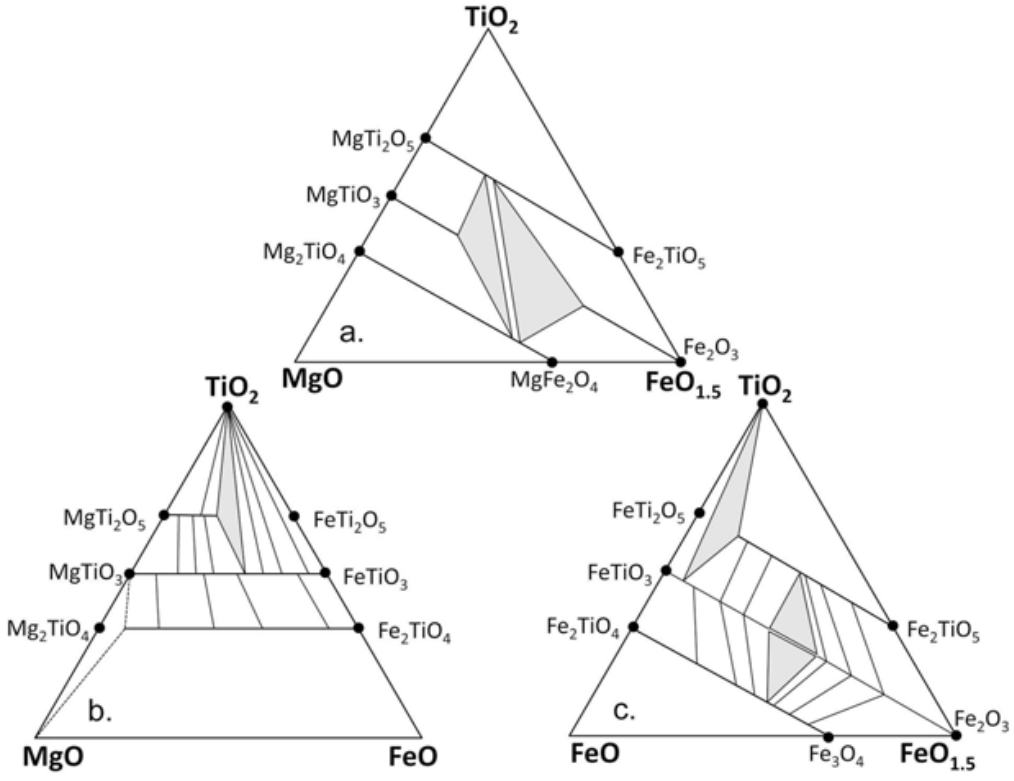
TiO2
MgTi2O5
MgTiO3
Mg2TiO4
Fe2TiO5
a.
Fe2O3
MgO
MgFe2O4
FeO1.5
TiO2
MgTi2O5
FeTi2O5
MgTiO3
FeTiO3
Mg2TiO4
Fe2TiO4
b.
MgO
FeO
TiO2
FeTi2O5
FeTiO3
Fe2TiO4
Fe2TiO5
c.
Fe2O3
FeO
Fe3O4
FeO1.5

Figure 8

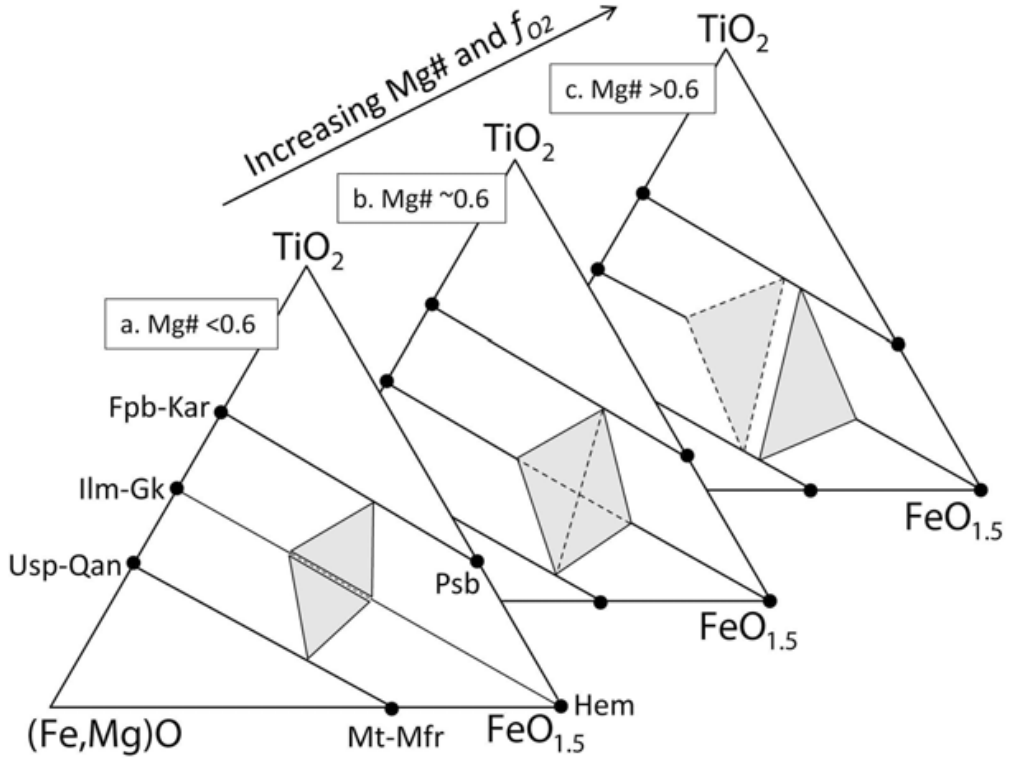
Increasing Mg# and f_{O2}
a. Mg# <0.6
b. Mg# ~0.6
c. Mg# >0.6
TiO_2
TiO_2
TiO_2
Fpb-Kar
Ilm-Gk
Usp-Qan
Psb
$FeO_{1.5}$
$FeO_{1.5}$
$FeO_{1.5}$
Hem
(Fe,Mg)O
Mt-Mfr